

# Research on inclination angle design of container loading and unloading platform based on sliding rail type three-dimensional wharf

Taiyang Li<sup>1</sup>, Mingjie Li<sup>2\*</sup>, Fangwei Zhang<sup>2</sup>, Muran Wang<sup>3</sup>, Mengchen Wang<sup>2</sup>

<sup>1</sup> School of Navigation and Shipping, Shandong Jiaotong University, Weihai, 264209, China

<sup>2</sup> School of International Business, Shandong Jiaotong University, Weihai, 264209, China

<sup>3</sup> School of Civil Engineering, Yantai University, Yantai, 264005, China

\*Correspondence to: Mingjie Li, Email: 201046@sdjtu.edu.cn

**Abstract:** At present, the traditional container terminal handling system has many problems, such as high energy consumption, high cost and low efficiency. Therefore, this study drew on the characteristics of "hump" transportation to design a sliding track type, three-dimensional wharf handling system. Meanwhile, considering the design problem of safety dip angle during the loading and unloading operation of the sliding rail terminal, this study constructed the calculation model of the optimal dip angle of the sliding rail operation. This provides a decision support for the improvement of the port handling system. Based on the aforementioned questions, this study first quantified the effects of temperature, humidity and container material. The correction factor for the friction coefficient was obtained. Secondly, combined with the classical mechanics theory, this study developed an optimal calculation model for the inclination of the sliding rail operation under the comprehensive effect of multiple factors. Finally, this study verified the rationality and safety of the optimal dip angle for a specific numerical case of a port. The results show that the safe inclination angle calculated in this case is 21.9°, which meets the requirements of safe operation. The applicability of the above research is verified.

**Keywords:** Three-dimensional wharf, Friction coefficient, Optimal inclination, Container handling, Safety

## 1. Introduction

With the rapid development of container terminals, the problems of high energy consumption, high cost and low efficiency of the traditional container terminal handling system have become increasingly prominent [1, 2]. To ensure the efficiency, environmental friendliness and safety of container handling operations, ports around the world, such as Yangshan Port, Qingdao Port in China and Hamburg Port in Germany, are actively working on the

transforming and upgrading of traditional terminals to automated terminals [3, 4]. However, there are also many problems in the process of construction, transformation and upgrading. Among them, the most important is the safety of containers loading and unloading. By consulting the relevant literature, the research on three-dimensional wharf mainly focuses on model construction, optimal design and efficiency, and safety analysis. In contrast, there are relatively few researches on the optimal inclination of the slide rail operation. In order to improve

Received: Oct.8, 2024; Revised: Nov.21, 2024; Accepted: Dec.2, 2024; Published: Dec.17, 2024

Copyright © 2024 Mingjie Li, et al.

DOI: <https://doi.org/10.55976/dma.3202513131-13>

This is an open-access article distributed under a CC BY license (Creative Commons Attribution 4.0 International License)  
<https://creativecommons.org/licenses/by/4.0/>

the safety and efficiency of three-dimensional wharf loading and unloading, this study analyzed the safety dip angle of slide rail operation. Firstly, an automated container rail transport system was presented in this study. Secondly, to ensure transportation safety, this study calculated the optimal inclination between the glide slope and the ground. Finally, the rationality of this inclination model was proved based on a specific numerical case. The study of the optimal angle is beneficial to improving the safety, efficiency and overall benefit of container handling.

## 1.1 Relevant studies

At present, lots of researches on three-dimensional wharves mainly focus on three aspects: the construction of a three-dimensional wharf model, the optimization of the design of a three-dimensional wharf, and the analysis of the efficiency and safety of a three-dimensional wharf.

Concerning the model construction of a three-dimensional wharf, Bielli et al. (2006) constructed a container terminal simulation model and gave a component architecture implemented in Java to study the methods of improving the efficiency of the port [5, 6]. Subsequently, Zhang (2008) proposed a modeling method and evaluation system for a three-dimensional rail network transmission system in a container terminal [7, 8]. Later, Pan et al. (2011) adopted the object-oriented stochastic Petri net modeling method to achieve the purpose of hierarchical modeling for the complex structure of the three-dimensional rail conveying system of a container terminal [9]. Next, Shi et al. (2013) proposed a new hybrid allocation algorithm for three-dimensional track equipment in automated container terminals [10]. Additionally, Roy et al. (2016) proposed a model using a load-dependent server that captures the interaction between the number of vehicles in a transit segment and the effective vehicle speed [11]. On the other hand, Zhao and Liu (2022) studied the design of a three-dimensional automated storage yard and the overall layout of the wharf [12].

As for the optimization of three-dimensional terminals, in the early years, Hartmann (2004) introduced a method to generate the scene of the container terminal, which is used as the input data of the simulation model to solve the optimization problem in the logistics of the container terminal [13]. Subsequently, Zhou et al. (2013) used the hybrid flow shop scheduling strategy to study the optimization strategy of the three-dimensional rail terminal transmission system and combined it with the genetic algorithm to simulate the scheduling strategy [14]. In recent years, Gharehgozli et al. (2020) summarized the future container terminals and listed the strategic and tactical problems in the layout design that need to be solved in relevant research [15]. Next, Muravev (2021) optimized the main parameters of the multimodal transport terminal in two stages by using the Anylogic simulation platform to realize the effective operation of

the multimodal transport terminal system in the port [16]. Recently, Hu et al. (2022) designed a genetic algorithm framework for efficient and low-carbon berth allocation in bulk cargo terminals [17].

In terms of the efficiency and safety analysis of the three-dimensional terminal, Yang et al. (2016) first used the decision making method to evaluate the main risk factors of container handling in Kaohsiung port, Taiwan [18]. Subsequently, Fang (2018) proposed a scheme of arranging the canopy in the U-shaped, which enables the loading and unloading of the bulk grain wharf on rainy days in rainy areas, and effectively reduces the imbalance coefficient, operating cost and difficulties in production organization in the operation area [19]. In recent years, based on the energy consumption during the cyclic operation of various equipment in the wharf, Wang et al. (2019) built a model to estimate the carbon emission of a wharf, which provides a decision-making support for the layout of sustainable development [20]. Next, by analyzing multimodal transport and its impact on port efficiency, Abuaisha et al. (2020) proposed a new layout of the container terminal in the port to reduce the port operation and production costs [21]. Recently, inspired by the excellent performance of deep learning in image recognition, Li et al. (2022) proposed a classification method for similar weather scenes in the terminal area based on improved deep convolution embedded clustering, which uses the combination of encoding layer and decoding layer to reduce the dimension of weather images [22].

In summary, the aforementioned researches mainly aim at constructing and optimizing the container transportation system for traditional three-dimensional wharf. However, research on the sliding rail container handling system of the three-dimensional wharf is less. Therefore, this study aims to develop a sliding rail container handling system. The best safety dip angle is determined by force analysis and potential energy transformation. It provides support to improve the efficiency and safety of container handling.

## 1.2 Objectives and contributions

The purpose of this research is to solve the problems of high energy consumption, high cost and low efficiency of the traditional container terminal loading and unloading system. Based on the advantages of "hump" transportation, a rail-type container handling system was designed in this research [23]. Meanwhile, to solve the design problem of the safe inclination angle of the slide rail, this study constructed a calculation model for the optimal inclination angle considering factors such as temperature and rain. In this way, it supports the transformation and upgrading of the loading and unloading system of the traditional container terminal.

The contributions of this study are as follows. First, a new type of three-dimensional slide-rail container handling system was designed and optimized in this study.

The handling system takes advantages of the "hump" transportation of the train track and uses the gravitational potential energy to convert the kinetic energy of the transportation container. It solves the problems of high transportation costs and high energy consumption of traditional small and medium-sized terminals. Secondly, this study comprehensively considered the effects of temperature, humidity and container material on friction. The factor integration method was used to determine a correction factor for the friction coefficient, which provides a theoretical basis for further research. Finally, based on the theory of classical mechanics and the law of conservation of energy, this study analyzed the movement process of the container on the slide rail. The model of the optimal inclination angle for slide rail operation was constructed considering various external factors.

This study is organized as follows. Section 2 explained the container unloading of the slideway three-dimensional wharf. Section 3 analyzed the factors that affect the container unloading system of the three-dimensional wharf, and elaborated the research ideas of this study. In Section 4, the two factors that affect the friction coefficient were quantified in the form of modified variables, and the calculation formula of the modified friction coefficient was extracted. By analyzing the force combined with the law of energy conservation and the inclination formula, the optimal inclination correction formula of the slide and the ground were extracted considering various factors. Section 5 verified the actual situation of the terminal. Finally, conclusions were drawn with future study directions indicated in Section 6. The framework of this study is shown in Figure 1.

## 2. Instructions of three-dimensional wharf

### 2.1 Layout of a stereoscopic wharf

This study drew on the characteristics of railway "hump" transportation, e.g. the principle of converting gravitational potential energy into kinetic energy of transport containers, and proposed a sliding rail-type unloading system for a three-dimensional wharf [24, 25]. The layout of the sliding rail container handling system was arranged as follows. First, in the part of the seaside track, this study adopted the cross three-dimensional structure. This structure is equipped with three layers of slip platform, according to the container stowage and loading and unloading requirements from cargo owner for a reasonable scheduling. These links will reasonably divert containers according to the loading and unloading orders. Secondly, in the land side track part, the inner truck reaches the position of the loading and unloading line at the front of the designated terminal. The truck and container are precisely docked point-to-point. And the container is transported along the peripheral, annular, three-dimensional track to the designated height of sliding platform. Finally, the container is loaded and transported through the shore bridge. The overall layout of the rail-type three-dimensional wharf is shown in Figure 2 and Figure 3.

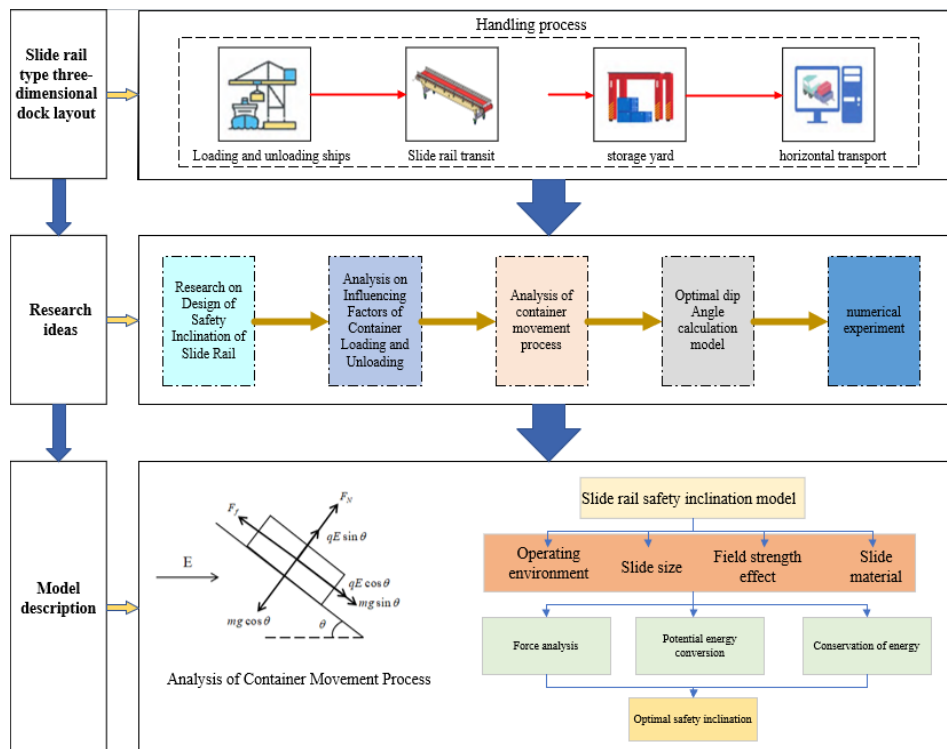


Figure 1. A research framework

## 2.2 Three-dimensional wharf production process

This study aims to provide new modeling ideas for the low-carbon transformation of port enterprises. Therefore, in this paper, it is assumed that the containers in the loading and unloading process are empty containers. During the unloading process, the three-dimensional wharf with sliding rail first uses the quay crane to unload the container from the ship and puts it on the slipping platform of the quay crane. Considering transportation safety, the containers' exterior are appropriately washed to reduce the large amount of impurities attached to the container surface during transportation and handling, while ensuring no damage to the cargo. Then, the loading and unloading equipment gives the container a constant force and pushes it to the three-dimensional interactive rail. The three-dimensional wharf uses the height difference to convert the gravitational potential energy into kinetic energy. There is no need for the assistance of other machinery during transportation. After the container enters a designated area, the container is moved forward by an electrically operated track system. As a result, the container is subjected to a uniform magnetic field during this process. This continues until the container is transported to the starting point of the yard, which

corresponds to the corresponding track. The horizontal transportation machinery picks up the containers placed at the end of the track and transports them to the designated storage location. During this process, a cooling device is installed under the system to reduce the heat generated by the sliding of the container and to ensure safety during transportation. After the stacking plan of yard is confirmed to be correct, the horizontal transportation machinery will unload the containers to the designated position. At this point, the uploading process of container will be completed in a three-dimensional terminal.

The method of rail slip is used for the entire container transportation process. The containers are delivered safely and efficiently to the container terminal or railroad crossing [26]. During the packing process, the truck drives to the corresponding yard crossing. The sliding platform uses the height difference to slide the container to the appropriate quay crane location for container unloading. On the one hand, this process reduces the use of mechanical equipment, which is conducive to reducing carbon emissions. On the other hand, it is beneficial to reduce the container turnover rate and reduce the time for the container to travel from the quay crane to the container yard.

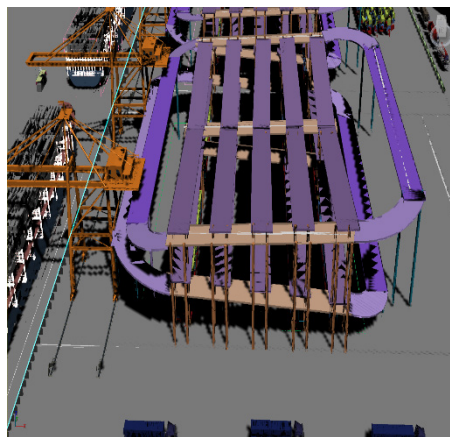


Figure 2. View of slide rail of the stereoscopic wharf

## 3. Research ideas and factor analysis

### 3.1 Analysis of influencing factors of container loading and unloading in three-dimensional wharf

Based on literature analysis, this study explored the influencing factors of container loading and unloading in three-dimensional wharf. The details are as follows.

(i) Operating environment: During container loading and unloading, both humidity and temperature can change the friction factor between the container and the skid.

Consequently, this leads to a change in the optimum angle of inclination between the slide and the ground [27].

(ii) Container material: Different materials of containers lead to different friction coefficients between slideways and containers, which affect the friction between slideways and containers [28].

(iii) Scale of the slide: The height of the slide affects the gravity potential energy of the container and the width of the slide affects the number of containers that can be loaded and unloaded. Both factors affect the calculation of the inclination [29].

(iv) Field strength: Due to the different types of goods

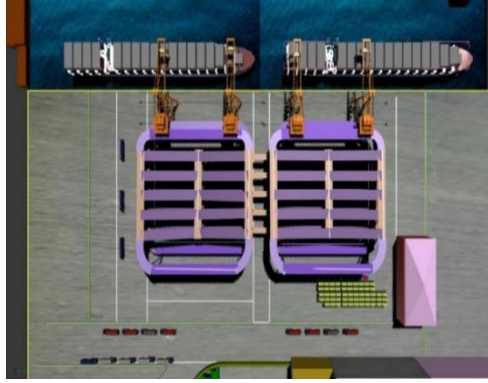


**Figure 3.** Model diagram of the stereoscopic wharf

loaded in containers, some goods are affected by electromagnetic fields. As a result, the external force acts on the container and thus changes the overall force of the container [30].

### 3.2 Research problems and ideas

In this study, it is found that one of the key factors affecting the efficiency and safety of container transportation is the design of the inclination of the slide rails. Therefore, this study comprehensively considered external factors such as weather and precipitation and finally extracted the optimal inclination model for slide rail operation. Firstly, this study quantitatively analyzed the four influencing factors of operating environment, container material, slide scale and field strength. Secondly, combined with the classical mechanical formula and the theorem of energy conservation, the movement distance of the container on the slide is determined in two stages, respectively. Finally, using the relationship between the height of the slideway and the length of the slideway in combination with the formula for inclination angle, this study extracted the optimal formula for inclination angle of the slideway and the ground during container loading and unloading, considering a variety of factors. At the same time, combined with the actual survey data of a port, the optimal inclination angle of the slide rail

safety production proposed in this study is analyzed and verified.

## 4. Model construction

In this section, this study comprehensively considered external factors such as the operating environment, container material, slideway scale, and the field strength. Then, combined with Newton's law of motion and the law of conservation of energy, the movement process of the container on the sliding rail was analyzed. Finally, combined with the inclination formula, the optimal calculation model for the inclination of the slide rail operation was extracted.

### 4.1 Friction coefficient operator

When transporting containers on slide rails, different operating environments and the choice of container material affect the value of the friction coefficient. The parameters in this study are listed in Table 1 to simplify the research. And the influence of different container materials on the friction of the slide rail was investigated in this study. By using the method of factor integration, the humidity and temperature correction functions were refined, then we got

$$\sigma^* = \left[ \frac{1}{\pi} \arctan \left( \frac{N^*}{N} \right) + \frac{1}{2} \right] \text{sgn}(N^* - N),$$

$$\text{sgn}(N^* - N) = \begin{cases} 1, & (N^* - N \geq 0); \\ 0, & (N^* - N < 0), \end{cases} \quad \sigma = \text{sgn}(\sigma^*) = \begin{cases} \sigma^*, & (N^* - N \geq 0); \\ A, & (N^* - N < 0). \end{cases}$$

(1)

$$\rho = g(T) = \begin{cases} \frac{2}{\pi} \arctan(T^* - T) + 1, & (T \leq T^*); \\ \frac{1}{\pi} \arctan \left( \frac{T^*}{T} \right) + \frac{1}{2}, & (T > T^*). \end{cases}$$

(2)

In Eq. (1),  $\text{sgn}(N^* - N)$  represents the impact of the precipitation threshold on the friction coefficient. Considering that the influence of humidity on the friction coefficient has an upper limit, that is, when the precipitation reaches the threshold value of  $N^*$ , it has the greatest influence. Even if the precipitation continues to increase, the friction coefficient still maintains at the maximum influence value. However, taking the actual situation into account, at this time, the container is additionally subject to a large rainwater thrust, which

balances out the friction force. Therefore, the friction force at this time is 0, that is, the friction coefficient is 0. However, considering the excessive danger in practical applications, a lower limit value for absolute safety was set in this study, which is denoted by  $A$ . In case of excessive precipitation, the friction coefficient decreases to this safety threshold. At this point, loading and unloading work is terminated for safety. To sum up, the operator of the modified friction coefficient is defined as

$$\mu = (\rho)^{\omega_1} \cdot (\sigma)^{\omega_2} \cdot \mu = [g(T)]^{\omega_3} \cdot \left[ \frac{1}{\pi} \arctan\left(\frac{N^*}{N}\right) + \frac{1}{2} \right] \text{sgn}(N^* - N)^{\omega_4} \cdot \lambda^* \cdot \mu_i. \quad (3)$$

## 4.2 Calculation model of optimal inclination of slide rail operation

In unloading operation, the container on the slide rail is subjected to the supporting force, the force of gravity, the friction force and the force of the electric field. The force analysis of the container movement process is shown in Figure 4. In this study, the movement process of the container on the slide rail is divided into two stages. The details are as follows. First, before the container enters the electromagnetic field area, the potential energy is converted into kinetic energy to provide power. At this time, the container initially moves in a straight line with uniform acceleration on the gentle sliding rail while being subjected to the action of the friction force at the same time. Later, when the potential energy is no longer sufficient to generate enough power, the container moves at a uniform deceleration until the speed is equal to that of the slideway. At this point, the container moves at a uniform speed. Then it enters the electromagnetic field and begins to be affected by the uniform magnetic field. The container continues to move at a constant speed until it leaves the slide rail. The steps of model construction are as follows.

**Step 1:** Before the container entering the electromagnetic field, the gravitational potential energy is converted into kinetic energy. Meanwhile, the friction force is also doing work. The container first performs a uniform acceleration motion on the slideway and then performs a uniform deceleration motion until it reaches the final stable speed and performs a uniform motion. The analysis of the potential energy is shown in Figure 5. Among them,  $v$  is the final stable speed of the container on the slide;  $h$  is the height of the slide from the ground;  $h_1$  is the height of the container from the ground when it reaches the stable speed on the slide;  $S_1$  is the distance that the container moves on the slide rail before its speed stabilized;  $m$  is the weight of the container;  $g$  is the gravitational acceleration of the slide location;  $q$  is the amount of charge carried by the container and its loaded goods;  $E$  is the electric field intensity of

the slide location;  $\theta$  is the angle between the slide and the ground;  $F_f$  is the friction between the container and the slide;  $F_N$  is the supporting force of the slide to the container, and  $\mu$  is the friction coefficient between the slide and the container. Then, according to the law of conservation of energy and Newton's law of motion, Eq. (4) is obtained.

$$\begin{cases} m \cdot g \cdot (h - h_1) = \frac{m \cdot v^2}{2} + \mu \cdot F_N \cdot S_1; \\ F_N + q \cdot E \cdot \sin \theta - m \cdot g \cdot \cos \theta = 0; \\ h - h_1 = S_1 \cdot \sin \theta. \end{cases} \quad (4)$$

Simultaneous Eq. (5) is obtained as

$$S_1 = \frac{m \cdot v^2}{2 \cdot \left[ \frac{m \cdot g \cdot \sin \theta - \mu \cdot (m \cdot g \cdot \cos \theta - q \cdot E \cdot \sin \theta)}{\mu \cdot (m \cdot g \cdot \cos \theta - q \cdot E \cdot \sin \theta)} \right]}. \quad (5)$$

**Step 2:** According to the theorem of kinetic energy, the Lorentz force does no work after the container entering the action area of electromagnetic field. The electric force and gravity perform positive work, while friction does negative work [31]. In unloading operation, the container overcomes the friction force on the sliding rail to do work. In this process, the mechanical energy is converted to the internal energy, and the container moves at a uniform speed. It is assumed that the expected movement time of the container moving at a uniform speed on the slideway is  $t$ . Therefore, according to Newton's law of motion, the working process at this stage is shown in Eq. (6). The speed and distance of the uniform motion of the container are calculated in Eq. (7) and Eq. (8).

$$\begin{cases} F = Bqv; \\ B \cdot q \cdot v = m \cdot g \cdot \cos \theta - q \cdot E \cdot \sin \theta. \end{cases}$$

(6)

$$v = \frac{mg \cos \theta - qE \sin \theta}{Bq},$$

(7)

$$S_2 = vt = \frac{mg \cos \theta - qE \sin \theta}{Bq} \cdot t.$$

(8)

**Step 3:** To ensure the safety and efficiency of the container during transportation on the slide rail, the movement speed of the container is set as  $v = 1\text{m/s}$  [32]. Then, Eq. (9) is obtained by combining Eq. (6) and Eq. (7).

$$Bq = mg \cos \theta - qE \sin \theta.$$

(9)

$$S_1 = \frac{m}{2 \cdot [m \cdot g \cdot \sin \theta - \mu \cdot (m \cdot g \cdot \cos \theta - q \cdot E \cdot \sin \theta)]}.$$

(10)

$$S_2 = vt = t.$$

(11)

Bring Eq. (9) into Eq. (10) to get

$$S_1 = \frac{m}{2 \cdot (m \cdot g \cdot \sin \theta - \mu \cdot B \cdot q)}.$$

(12)

**Step 4:** From the relationship among height  $h$ , distance  $S$  and included angle  $\theta$ , the included angle  $\theta$  between slide and the ground is calculated.

$$S = S_1 + S_2 = \frac{m}{2 \cdot (m \cdot g \cdot \sin \theta - \mu \cdot B \cdot q)} + t.$$

(13)

$$\theta = \arcsin \left[ \left[ \left( \frac{2 \cdot m \cdot g \cdot h - m}{+2 \cdot \mu \cdot B \cdot q \cdot t} \right) + \sqrt{\left( \frac{m - 2 \cdot m \cdot g \cdot h}{-2 \cdot \mu \cdot B \cdot q \cdot t} \right)^2 - \left( \frac{16 \cdot m \cdot g \cdot t}{\mu \cdot B \cdot q \cdot h} \right)} \right] \cdot (4 \cdot m \cdot g \cdot t)^{-1} \right].$$

(19)

$$h = S \cdot \sin \theta.$$

(14)

Bring Eq. (13) into Eq. (14) to get

$$h = \left[ \frac{m}{2 \cdot (m \cdot g \cdot \sin \theta - \mu \cdot B \cdot q)} + t \right] \cdot \sin \theta.$$

(15)

Simplify Eq. (14) to obtain

$$2 \cdot m \cdot g \cdot t \cdot (\sin \theta)^2 + (m - 2 \cdot m \cdot g \cdot h - 2 \cdot \mu \cdot B \cdot q \cdot t) \cdot \sin \theta + 2 \cdot \mu \cdot B \cdot q \cdot h = 0.$$

(16)

Since the target quantity has only one angle, and the other variables are regarded as parameters. Therefore, the function  $f(x)$  belonging to  $\sin \theta$  is constructed. And if

$$A = 2 \cdot m \cdot g \cdot t$$

$$B = (m - 2 \cdot m \cdot g \cdot h - 2 \cdot \mu \cdot B \cdot q \cdot t)$$

$$C = 2 \cdot \mu \cdot B \cdot q \cdot h$$

there is

$$f(x) = Ax^2 - Bx + C$$

(17)

According to the formula for finding the root of quadratic function, when  $f(x) = 0$ ,  $x = \sin \theta$ , Eq. (16) is obtained. At this point, Eq. (16) has two solutions such as Eq. (17).

$$\sin \theta = \frac{-B \pm \sqrt{B^2 - 4 \cdot A \cdot C}}{2 \cdot A}.$$

(18)

In Eq. (18), it holds  $\Delta = B^2 - 4 \cdot A \cdot C \geq 0$ ,  $[(m - 2 \cdot m \cdot g \cdot h - 2 \cdot \mu \cdot B \cdot q \cdot t)^2 - 16 \cdot m \cdot g \cdot t \cdot \mu \cdot B \cdot q \cdot h] \geq 0$ .

Since the inclination is  $\theta > 0$ , the negative solution

$$\sin \theta = \frac{-B - \sqrt{B^2 - 4 \cdot A \cdot C}}{2 \cdot A} \text{ is rounded off,}$$

Bring Eq. (3) into Eq. (19) to get

$$\theta = \arcsin \left[ \frac{\begin{matrix} \left( m - 2 \cdot m \cdot g \cdot h - 2 \cdot [g(T)]^{\omega_1} \right) \\ \cdot \left[ \frac{1}{\pi} \arctan \left( \frac{N^*}{N} \right) + \frac{1}{2} \right]^{\omega_2} \cdot \lambda^* \\ \text{sgn}(N^* - N) \cdot B \cdot q \cdot t \cdot \mu_i \end{matrix}}{\begin{matrix} \left( m - 2 \cdot m \cdot g \cdot h - 2 \cdot [g(T)]^{\omega_1} \right)^2 \\ \cdot \left[ \frac{1}{\pi} \arctan \left( \frac{N^*}{N} \right) + \frac{1}{2} \right]^{\omega_2} \cdot \lambda^* \\ \text{sgn}(N^* - N) \cdot B \cdot q \cdot t \cdot \mu_i \end{matrix}} - \frac{\begin{matrix} \left( 16 \cdot m \cdot g \cdot \lambda^* [g(T)]^{\omega_1} \cdot h \right) \\ \cdot \left[ \frac{1}{\pi} \arctan \left( \frac{N^*}{N} \right) + \frac{1}{2} \right]^{\omega_2} \\ \text{sgn}(N^* - N) \cdot B \cdot q \cdot t \cdot \mu_i \end{matrix}}{\left( 4 \cdot m \cdot g \cdot t \right)^{-1}} \right] \quad (20)$$

### 4.3 Supplement and explanation

Firstly, this study refined the modified friction coefficient operator under the influence of humidity, temperature and other factors. Secondly, combined with the classical mechanical model and the theorem of energy conservation, the moving distance of the container on the slide was calculated. Finally, combined with the inclination formula, the optimal calculation model for the inclination of the slide rail was extracted under the four influencing factors of operating environment, container material, slide size and field strength. Considering the special circumstances, supplements and explanations are given in this section.

**Table 1.** Symbolic representation

Parameter	Meaning
$\mu$	Friction coefficient
$\lambda$	Environment of transporting containers
$i$	Material of container
$\rho$	Temperature influence coefficient
$\sigma$	Humidity influence coefficient
$\omega_1$	Weight of temperature influence $\omega_1 = 1/2$
$\omega_2$	Weight of humidity influences $\omega_2 = 1/2$
$T$	Daily average temperature
$N$	Daily average precipitation
$T^*$	Normal temperature, the default temperature in this study is 20 °C
$N^*$	The maximum precipitation threshold is 40mm by default in this study
$\lambda^*$	The coefficient of other influencing factors is 1 by default in this study

For Eq. (3), the inferences and properties are as follows.

**Inference 1:** When the precipitation  $N$  approaches 0, the humidity correction coefficient is

$$\lim_{N \rightarrow 0} \sigma = \lim_{N \rightarrow 0} \left[ \frac{1}{\pi} \arctan \left( \frac{N^*}{N} \right) + \frac{1}{2} \right] \text{sgn}(N^* - N) = 1.$$

**Property 1:** When  $N$  is 0, it is regarded as  $N$  approaching 0. At this time, it means that the rainfall is 0, that is, humidity has no effect on the friction coefficient  $\mu$  and then the humidity correction coefficient  $\sigma$  is 1.

**Inference 2:** When the temperature  $T = T^*$ , the temperature correction factor is

$$\rho = g(T) = \frac{2}{\pi} \arctan(T^* - T) + 1 = 1.$$

**Property 2:** When  $T = T^*$ , it means that the average temperature of the day is the same as the normal temperature, that is  $T^* - T = 0$ , e.g., temperature does not affect the friction coefficient  $\mu$  so the temperature correction coefficient  $\sigma$  is 1.

**Inference 3:** When the precipitation  $N$  exceeds the precipitation threshold  $N^*$  the humidity correction coefficient is

$$\sigma = \left[ \frac{1}{\pi} \arctan \left( \frac{N^*}{N} \right) + \frac{1}{2} \right] \text{sgn}(N^* - N) = A.$$

**Property 3:** When the precipitation  $N$  exceeds the precipitation threshold  $N^*$  and considering the thrust effect of large precipitation on the container and the safety factors of wharf loading and unloading, the friction coefficient  $\mu$  is  $A$ .

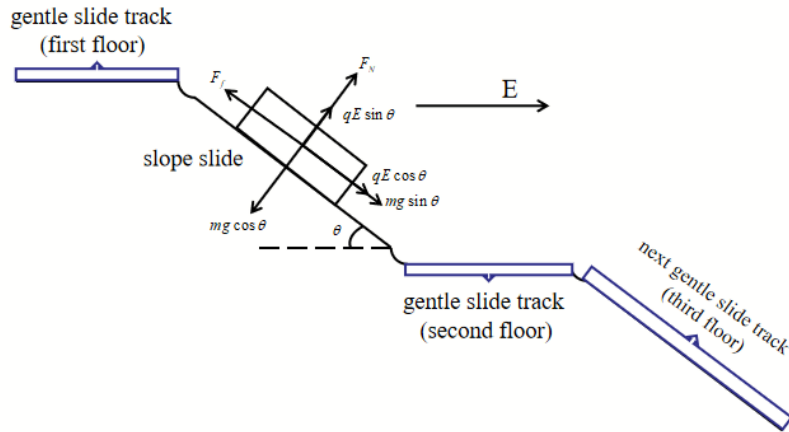


Figure 4. Stress analysis of container analysis

## 5. Data collection and analysis

### 5.1 Information collection

Based on the model in Section 4, data from a port were collected and validated in this study. First, the influence of the operating environment is particularly critical for the design of safe inclination. Therefore, this study focuses on the design of the inclination angle of the slide rail under different temperatures and different precipitation. The survey data of temperature and precipitation in the city where a port is located are shown in Figure 6 and Figure 7. Secondly, the material of the container and the scale of the slideway also affect the calculation of the optimal inclination angle of the slideway operation. At the same time, the containers used in this port are all steel containers with a slideway height of 10 meters. Finally, the fact that the magnitude of the electric field force also has a certain influence on the design of the inclination angle was taken into account in this study. According to the measurement, the electric field force of a port is 200000 N. The final detailed statistics are shown in Table 3.

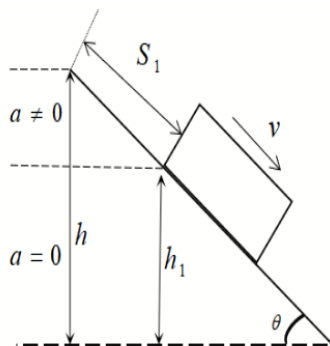


Figure 5. Potential energy analysis

### 5.2 Numerical calculation

In this study, the friction coefficients of four common container materials and the rubber slide rail determined based on literature research were listed. The specific values are shown in Table 2 [33]. Based on the calculation model for the optimal inclination of the slide rail operation in Section 4, Table 3 was used in the model for data analysis. The correction coefficients for humidity and temperature were calculated in sequence. Then the correction coefficients for humidity and temperature were substituted into the friction coefficient operator to calculate the corrected friction coefficient. Finally, the optimal inclination angle between the slide and the ground was calculated under the joint influence of the operating environment, the container material, the slide scale and the field strength. The specific steps for calculation are as follows.

**Step 1:** Substitute  $N = 15\text{mm}$ ,  $N^* = 40\text{mm}$  into Eq. (1), and the humidity correction coefficient is

$$\sigma = \left[ \frac{1}{\pi} \arctan \left( \frac{N^*}{N} \right) + \frac{1}{2} \right] \text{sgn} (N^* - N) = 0.89.$$

**Step 2:** Substitute  $T = 24^\circ\text{C}$ ,  $T^* = 20^\circ\text{C}$  into Eq. (2), and the temperature correction coefficient is

$$\rho = \frac{1}{\pi} \arctan \left( \frac{T^*}{T} \right) + \frac{1}{2}, (T > T^*) = 0.72.$$

**Step 3:** Substitute  $\sigma = 0.89$ ,  $\rho = 0.72$ ,  $\mu_i = 0.7$  into Eq. (3), the friction coefficient can be obtained as

$$\mu = (\sigma)^{\omega_1} \cdot (\rho)^{\omega_2} \cdot \lambda^* \cdot \mu_i = 0.56$$

**Step 4:** Substitute  $m = 30000 \text{ kg}$ ,  $h = 10\text{m}$ ,  $g = 10\text{m/s}^2$ ,  $t = 240\text{s}$ ,  $Bq = 200000 \text{ N}$  into Eq. (19), the best inclination angle is  $\theta = 21.9^\circ$ .

According to relevant information, the inclination angle of an ordinary belt conveyor is generally not greater than 30°, taking into account the properties of the materials [34]. The maximum inclination angle of materials with good fluidity and low friction will be smaller. According to the aforementioned calculation, the optimal inclination angle between the slide and the ground under the joint influence of the operating environment, container material, slide size, and field strength is 21.9°, which meets requirements for the port safety production.

**Table 2.** Friction coefficient between containers of different materials and rubber slideways

Container material	Friction coefficient
Steel container	$\mu_1 = 0.7$
Aluminum alloy container	$\mu_2 = 0.26$
FRP container	$\mu_3 = 0.35$
Aluminum container	$\mu_4 = 0.87$

**Table 3.** Layout parameters of a port

Parameter	Numerical value	Company
Container weight (Empty load of 10 standard containers)	30000	kg
Slide height	10	m
Electric field force	200000	N
Single delivery time of container	240	s
Annual average minimum temperature	-3	°C
Annual average maximum temperature	28	°C
Annual average minimum rainfall	13	mm
Annual average maximum rainfall	131	mm
Daily average temperature	24	°C
Daily precipitation	15	mm

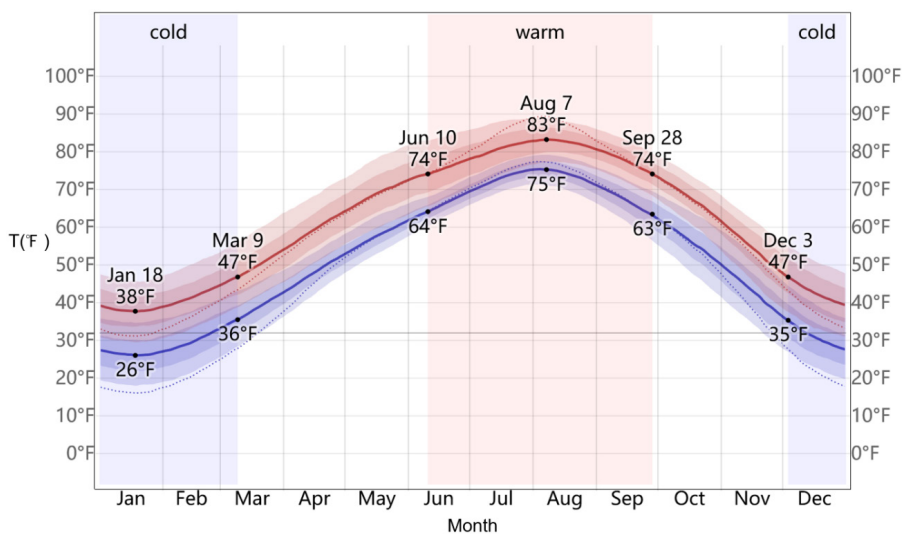


**Figure 6.** Average temperature change trend of a port in 2021

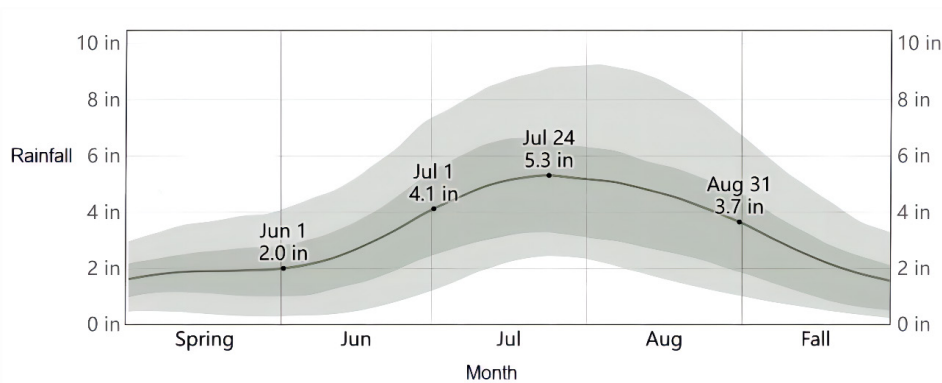


**Figure 7.** Average rainfall change trend of a port in 2021

## 6. Conclusion

Based on the characteristics of railway "hump" transportation, this research proposed a design for container unloading from sliding rail in three-dimensional dock. The design shows that the inclination angle of the slide is one of the key factors for the efficiency and safety of container transportation. Therefore, given the optimal inclination angle, this study constructed a calculation model of the optimal inclination angle for the sliding rail operation. The significance of this study is to provide a support for the design for the container unloading container in slideway three-dimensional wharf. The research innovation is mainly reflected in the following three points.

First, this study focuses on the optimization of container unloading operation in the three-dimensional terminal, it designed and optimized a new system for container handling in three-dimensional sliding rail. The handling system was established by drawing inspiration from the "hump" transportation of the train track. It solves the problems of high transportation costs and high energy consumption of traditional small and medium-sized terminals.

Secondly, to make the results more realistic, the effects of temperature, humidity and container material on friction were considered. The operator for friction coefficient correction was extracted.

Thirdly, based on the theory of classical mechanics and the law of conservation of energy, the movement process of the container on the slide rail was analyzed in this study. Then, combined with the inclination angle formula, the optimal model for inclination angle of the slide rail operation was constructed.

However, there are a limits of this study. It did not consider the tilting of fully loaded containers during transportation, and the impact of the electric field on the cargo if the container is fully loaded was also ignored. Besides, since the purpose of this study is to provide new modeling ideas, the actual cost has not been taken into account. In the future, we will comprehensively consider the above factors, computer software is further used to simulate and optimize the three-dimensional dock unloading system to achieve the purpose of practical application.

## Credit authorship contribution statement

Taiyang Li: methodology, writing-original draft; Mingjie Li: writing-review, validation; Fangwei Zhang: conceptualization, writing-review; Muran Wang: editing, validation; Mengchen Wang: software, validation, investigation.

## Data availability

Data sharing is not applicable to this research as no new data were created or analyzed in this study.

## Conflicts of interest

The authors declare that no conflict of interest exists for the publication of this research. This research publication is approved by all authors.

## Funding statement

The research work conducted by Fangwei Zhang is funded by the Natural Science Foundation of Shandong Province (ZR2021MG003).

## References

- [1] Carlo H J, Vis I F A, Roodbergen K J. Seaside operations in container terminals: literature overview, trends, and research directions. *Flexible Services and Manufacturing Journal*. 2015; 27: 224-262. doi: 10.1007/S10696-013-9178-3.
- [2] Younis G, Kamar L B, Attya H. Development strategy of the port said container terminal. *NAŠE MORE: znanstveni časopis za more i pomorstvo*. 2010; 57(1-2): 1-17.
- [3] Song L, Ravesteijn W. Responsible port innovation in China: the case of the Yangshan port extension project. *International Journal of Critical Infrastructures*. 2015; 11(4): 297-315. doi: 10.1504/IJCIS.2015.073841.
- [4] Zhou Q, Jiao Z, Huang Z, et al. Wear-resistant CrCoNi nanocrystalline film via friction-driven surface segregation. *Acta Materialia*. 2024; 279: 120299. doi: 10.1016/j.actamat.2024.120299.
- [5] Bielli M, Boulmakoul A, Rida M. Object oriented model for container terminal distributed simulation. *European Journal of Operational Research*. 2006; 175(3): 1731-1751. doi: 10.1016/j.ejor.2005.02.037.
- [6] Zhou Q, Xia Q, Li Q, et al. Microstructure, mechanical and tribological properties of NbMoWTaAg refractory high entropy films with nano-layered self-organization. *Tribology International*. 2024: 109888. doi: 10.1016/j.triboint.2024.109888.
- [7] L. Zhang, X. F. Shi and Q. Lu. DEDS modeling method and evaluation of container terminal three-dimensional rail network transmission system. *Transportation and Computer*. 2008; 1: 49-54. doi: 10.3963/j.issn.1674-4861.2008.01.012.
- [8] Ren Y, Huang Z, Wang Y, et al. Friction-induced rapid amorphization in a wear-resistant (CoCrNi) 88Mo12 dual-phase medium-entropy alloy at cryogenic temperature. *Composites Part B: Engineering*. 2023; 263: 110833. doi: 10.1016/j.compositesb.2023.110833.

- [9] C. X. Pan, J. L. Wang, X. D. Zhao and Q. Lu. Tridimensional rail terminal transmission system modeling and simulation. *Computer Engineering and Applications*. 2011; 47(31): 230-233. doi: 10.3778/j.issn.1002-8331.2011.31.065.
- [10] X. F. Shi, L. L. Liang and Q. Lu. A new algorithm for hybrid allocation of three-dimensional track equipment in automated container terminal. *Journal of Wuhan University of Technology (Traffic Science and Engineering Edition)*. 2013; 37(04): 745-748. doi: 10.3963/j.issn.2095-3844.2013.04.018.
- [11] Roy D, Gupta A, De Koster R B M. A non-linear traffic flow-based queuing model to estimate container terminal throughput with AGVs. *International Journal of Production Research*. 2016; 54(2): 472-493. doi: 10.1080/00207543.2015.1056321.
- [12] Z. B. Zhao and W. Liu. Design of "zero turnover" automatic three-dimensional storage yard and general layout of wharf. *Water Transportation Engineering*. 2022; (02): 37-45. doi: 10.16233/j.cnki.issn1002-4972.20220125.011.
- [13] Hartmann S. Generating scenarios for simulation and optimization of container terminal logistics. *Or Spectrum*. 2004; 26(2): 171-192. doi: 10.1007/3-540-26686-0\_4.
- [14] Z. P. Zhou, M. L. Liang and C. X. Pan. Genetic algorithm based scheduling strategy for three-dimensional wharf transportation system. *Computer Engineering and Applications*. 2013; 49(12): 228-232. doi: 10.3778/j.issn.1002-8331.1204-0283.
- [15] Gharehgozli A, Zaerpour N, de Koster R. Container terminal layout design: transition and future. *Maritime Economics & Logistics*. 2020; 22: 610-639. doi: 10.1057/s41278-019-00131-9.
- [16] Muravev D, Hu H, Rakhmangulov A, et al. Multi-agent optimization of the intermodal terminal main parameters by using AnyLogic simulation platform: Case study on the Ningbo-Zhoushan Port. *International Journal of Information Management*. 2021; 57: 102133. doi: 10.1016/j.ijinfomgt.2020.102133.
- [17] Hu X, Ji S, Hua H, et al. An Improved Genetic Algorithm for Berth Scheduling at Bulk Terminal. *Computer Systems Science & Engineering*. 2022; 43(3). doi: 10.32604/csse.2022.029230.
- [18] Yang Y L, Ding J F, Chiu C C, et al. Core risk factors influencing safe handling operations for container terminals at Kaohsiung port. *Proceedings of the Institution of Mechanical Engineers, Part M: Journal of Engineering for the Maritime Environment*. 2016; 230(2): 444-453. doi: 10.1177/1475090214563859.
- [19] D. R. Fang. Handling technology scheme of inland bulk grain wharf in rainy areas. *Engineering and Construction*. 2018; 32(05): 717-718. doi: 10.3969/j.issn.1673-5781.2018.05.022.
- [20] Wang N, Chang D, Shi X, et al. Analysis and design of typical automated container terminals layout considering carbon emissions. *Sustainability*. 2019; 11(10): 2957. doi: 10.3390/su11102957.
- [21] Abu Aisha T, Ouhimmou M, Paquet M. Optimization of container terminal layouts in the seaport—Case of port of Montreal. *Sustainability*. 2020; 12(3): 1165. doi: 10.3390/su12031165.
- [22] Yuan L, Jin J, Xu Y, et al. Study on recognition method of similar weather scenes in terminal area. *Computer Systems Science and Engineering*. 2023; 44(2): 1171-1185. doi: 10.32604/csse.2023.027221.
- [23] Dick C T, Dimberger J R. Advancing the science of yard design and operations with the CSX hump yard simulation system. *Proceedings of the 2014 Joint Rail Conference*. 2014 Joint Rail Conference. Colorado Springs, Colorado, USA. 2014. V001T04A006. ASME. doi: 10.1115/JRC2014-3841.
- [24] Zhang J., Ioannou P A, Chassiakos A. Automated container transport system between inland port and terminals. *ACM Transactions on Modeling and Computer Simulation*. 2006; 16(2): 95-118. doi: 10.1145/1138464.1138465.
- [25] Başlamışlı S C, Ünlüsoy Y S. Optimization of speed control hump profiles. *Journal of transportation engineering*. 2009; 135(5): 260-269. doi: 10.1061/(ASCE)TE.1943-5436.0000002.
- [26] Tan C., He J., Wang Y. Storage yard management based on flexible yard template in container terminal. *Advanced Engineering Informatics*. 2017; 34: 101-113. doi: 10.1016/j.aei.2017.10.003.
- [27] Guo L., Wang J., Zheng J.. Berth allocation problem with uncertain vessel handling times considering weather conditions. *Computers & Industrial Engineering*. 2021; 158: 107417. doi: 10.1016/j.cie.2021.107417.
- [28] Chen F., Yu X. Issues and Countermeasures of Roll-on/Roll-off Transshipment for Track-Type Container Gantry Cranes. *Journal of Nanjing Institute of Industrial Technology*. 2017; 17(2): 7-9. doi: 10.15903/j.cnki.jniit.2017.02.003.
- [29] Liang Dawei. Technical Characteristics and Design Innovations of Track-Type Container Gantry Cranes. *China Equipment Engineering*. 2018; (15):174-175.
- [30] Chai Z., Cui Z., Xie H. Control of Interference from the Cable Electromagnetic Field on IGV Magnetic Pins at Automated Container Terminals. *Waterway Engineering*. 2022; (10): 199-203. doi: 10.16233/j.cnki.issn1002-4972.20220927.031.
- [31] Huynh N., Walton C M, Davis J. Finding the number of yard cranes needed to achieve desired truck turn time at marine container terminals. *Transportation Research Record*. 2004; 1873(1): 99-108. doi: 10.3141/1873-12.
- [32] Zhao Y. The slowest AC drive traction flat car in China - the conveyor subsystem of the customs container inspection system. *Electric Locomotive Technology*. 2000; (04): 21-22. doi: 10.16212/j.cnki.1672-1187.2000.04.008.
- [33] Liu J., Zhao Q. and Qi Z. Research on the integration

of electric locomotive technology, 5.0 M high mining height, fully mechanized mining, intensive and efficient technology. *Journal of Coal*. 2010; 35(11): 1783-1788. doi: 10.13225/j.cnki.jccs.2010.11.004.